

# The fate of fixed nitrogen in Santa Barbara Basin sediments during seasonal anoxia

Xuefeng Peng<sup>1,2,3</sup>, David J. Yousavich<sup>4</sup>, Annie Bourbonnais<sup>1</sup>, Frank Wenzhöfer<sup>5,6,7</sup>, Felix Janssen<sup>5,6</sup>, Tina Treude<sup>4,8</sup> and David L. Valentine<sup>2,3</sup>

5 <sup>1</sup>School of Earth, Ocean and Environment, University of South Carolina, 701 Sumter Street, Columbia, SC, USA

<sup>2</sup>Marine Science Institute, University of California, Santa Barbara, CA, USA

<sup>3</sup>Department of Earth Science, 1006 Webb Hall, University of California, Santa Barbara, CA, USA

<sup>4</sup>Department of Earth, Planetary, and Space Sciences, University of California Los Angeles, 595 Charles E. Young Drive East, Los Angeles, CA, USA

10 <sup>5</sup>HGF-MPG Joint Research Group for Deep-Sea Ecology and Technology, Alfred-Wegener-Institute, Helmholtz Centre for Polar and Marine Research, Am Handelshafen 12, Bremerhaven, Germany

<sup>6</sup>Max Planck Institute for Marine Microbiology, Celsiusstrasse 1, Bremen, Germany

<sup>7</sup>Department of Biology, HADAL Centre, University of Southern Denmark, Odense M, Denmark

<sup>8</sup>Department of Atmospheric and Oceanic Sciences, University of California Los Angeles, Math Science Building,  
15 520 Portola Plaza, Los Angeles, CA, USA.

*Correspondence to:* Xuefeng Peng ([xpeng@seoe.sc.edu](mailto:xpeng@seoe.sc.edu)) and David L. Valentine ([valentine@ucsb.edu](mailto:valentine@ucsb.edu))

## **Abstract.**

20 Despite long-standing interests in the biogeochemistry of the Santa Barbara Basin (SBB), there are no direct rate measurements of different nitrogen transformation processes. We investigated benthic nitrogen cycling using in-situ incubations with  $^{15}\text{NO}_3^-$  addition and quantified the rates of total nitrate ( $\text{NO}_3^-$ ) uptake, denitrification, anaerobic ammonia oxidation (anammox),  $\text{N}_2\text{O}$  production, and dissimilatory nitrate reduction to ammonia (DNRA). Denitrification was the dominant  $\text{NO}_3^-$  reduction process, while

25 anammox contributed 0 - 27% to total  $\text{NO}_3^-$  reduction. DNRA accounted for less than half of  $\text{NO}_3^-$  reduction except at the deepest station at the centre of the SBB where  $\text{NO}_3^-$  concentration was lowest.  $\text{NO}_3^-$  availability and sediment total organic carbon content appeared to be two key controls on the relative importance of DNRA. The increasing importance of fixed N retention via DNRA relative to fixed N loss as  $\text{NO}_3^-$  deficit intensifies suggests a negative feedback loop that potentially contributes to stabilizing the

30 fixed N budget in the SBB. Nitrous oxide ( $\text{N}_2\text{O}$ ) production as a fraction of total  $\text{NO}_3^-$  reduction ranged from 0.2% to 1.5%, which was higher than previous reports from nearby borderland basins. A large fraction of  $\text{NO}_3^-$  uptake was unaccounted for by  $\text{NO}_3^-$  reduction processes, suggesting that intracellular storage may play an important role. Our results indicate that the SBB acts as a strong sink for fixed nitrogen and potentially a net source of  $\text{N}_2\text{O}$  to the water column.

35

## 1 Introduction

Oxygen minimum zones (OMZs) in the world's ocean, whether they are formed naturally or induced by human activities, have been expanding in the past century (Horak et al., 2016; Oschlies et al., 2017; 40 Stramma et al., 2008). As oxygen ( $O_2$ ) concentration is one of the key controls on biogeochemical processes, including nitrogen (N) cycling, N biogeochemistry in OMZs has been extensively studied (Paulmier and Ruiz-Pino, 2009; Zehr, 2009). Denitrification, the reduction of nitrate ( $NO_3^-$ ) to dinitrogen gas ( $N_2$ ), and anaerobic ammonia oxidation (anammox), where nitrite ( $NO_2^-$ ) and ammonium ( $NH_4^+$ ) are converted into  $N_2$  by comproportionation are two major sinks of the oceanic fixed N budget (Gruber, 45 2008). These two processes are inhibited by the presence of  $O_2$  and sulfide, and their rates are sensitive to  $O_2$  at nanomolar concentrations (Dalsgaard et al., 2014; Joye and Hollibaugh, 1995; Caffrey et al., 2019). Because the last step of the sequential reduction of  $NO_3^-$  during denitrification,  $N_2O$  reduction, is the most sensitive to  $O_2$  (Zumft, 1997), the production of nitrous oxide ( $N_2O$ ) as a byproduct of denitrification is usually elevated under hypoxic conditions, i.e., in the presence of  $O_2$  (Firestone et al., 50 1980; Ji et al., 2015). Additionally, nitrification, i.e., the oxidation of  $NH_4^+$  and subsequently  $NO_2^-$  is another major source of  $N_2O$  in the ocean (Elkins et al., 1978), and the relative yield of  $N_2O$  from nitrification is high under low- $O_2$  conditions ( $<4 \mu M$ ) (Ji et al., 2018). Under  $O_2$  limitation, dissimilatory nitrate reduction to ammonia (DNRA) coupled to organic matter degradation is another important process that results in fixed N retention instead of removal (Burgin and Hamilton, 2007). When viewed as 55 competing processes, DNRA is favored over denitrification under  $NO_3^-$ -limited conditions where electron donors are in excess (Tiedje et al., 1983). Additionally, under sulfidic conditions, autotrophic DNRA coupled to sulfide oxidation can become a dominant pathway for  $NO_3^-$  reduction (Shao et al., 2011).

The Santa Barbara Basin (SBB) is one of the borderland basins off the southern part of the coast of 60 California and characterized by high export production (Thunell, 1998). Because the bottom water (maximum depth 586 m) in the SBB is separated from the area outside the basin by relatively shallow sills on the eastern end ( $\sim 200$  m deep) and the western end ( $\sim 475$  m deep),  $O_2$  concentrations at the basin's bottom is generally low and usually fluctuates between 1 and  $30 \mu M$  (Bograd et al., 2002; Goericke et al., 2015; Reimers et al., 1990; Sholkovitz and Gieskes, 1971; Myhre et al., 2018). During upwelling seasons

65 (winter and spring), water is advected from outside the basin and replenishes bottom water  $O_2$  in the SBB. However, high export production fuels  $O_2$  demand that maintains low  $O_2$  levels within the basin at depths below the deeper sill (Thunell, 1998). As a consequence, anoxia develops at the bottom of the SBB until the next upwelling event (Goericke et al., 2015), and large coverage of bacterial mats on the sea floor has been reported in the SBB (Valentine et al. 2016).

70

Using water column  $NO_3^-$  concentration data collected in the SBB by the California Cooperative Oceanic Fisheries Investigations (CalCOFI) along longitudinal transects (Koslow et al., 2010), Valentine et al. (2016) estimated the benthic  $NO_3^-$  uptake rate to be as high as  $11.7 \text{ mmol m}^{-2} \text{ d}^{-1}$ , which was one of the highest rates ever reported. However, the fate of the  $NO_3^-$  in the sediments remains unclear as there are  
75 no direct rate measurements of N cycling processes in the SBB. Indirect estimates using analysis of stable isotopes of water column  $NO_3^-$  suggests that benthic denitrification accounts for  $> 75\%$  of  $NO_3^-$  loss in the SBB, and the rates of benthic denitrification were estimated to be the highest among borderland basins in the eastern tropical North Pacific (Sigman et al., 2003). Benthic anammox is expected to occur in the SBB (Prokopenko et al., 2006), but the relative contribution of denitrification and anammox to  $N_2$   
80 production has not been assessed. In addition to different dissimilatory processes that reduce  $NO_3^-$ , the apparent  $NO_3^-$  drawdown could also be attributed to intracellular storage by both prokaryotes and microbial eukaryotes (Kamp et al., 2015; Bernhard et al., 2012; Schulz et al., 1999). With respect to  $N_2O$ , these other borderland basins are considered to be a weak sink (Townsend-Small et al., 2014). As the SBB stands out in terms of denitrification, it may be expected that SBB benthic cycling of  $N_2O$  is also  
85 unique.

To decipher the fate of  $NO_3^-$  taken up by SBB sediments, we performed in-situ incubations using benthic flux chambers with added  $^{15}NO_3^-$  along the bottom slope traversing north-south across the deeper portion of the SBB. By calculating the rates of  $N_2$  production by denitrification and anammox, total  $N_2O$   
90 production, and DNRA, we assess the overall rates of  $NO_3^-$  uptake and reduction rates. Accompanying geochemical data are used to explore the controls on the relative importance of  $NO_3^-$  retention via DNRA.

## 2 Materials and Methods

### 2.1 In situ incubations with benthic flux chambers

Remotely operated vehicle (ROV) Jason deployed automated benthic flux chambers (BFC) and conducted sediment push coring at seven stations (Fig. 1) in the SBB along a southern and a northern depth and O<sub>2</sub> gradient originating from the depocenter in the deepest point of the basin (Table 1). Station depth, latitude, and longitude were automatically generated by the Jason data processor using navigation data derived from the Doppler Velocity Log system and the ultrashort baseline positioning system. Bottom water O<sub>2</sub> concentration was determined using a Type 4831 O<sub>2</sub> optode sensor (Aanderaa Data Instruments AS, Bergen, NO) on the ROV and calibrated against Winkler titration measurements of seawater collected from Niskin bottles (Qin et al., 2022). Bottom water was collected using Niskin bottles and stored frozen at -30°C until lab analysis for nitrate (NO<sub>3</sub><sup>-</sup>) concentration following the spectrophotometric method described by (García-Robledo et al., 2014).

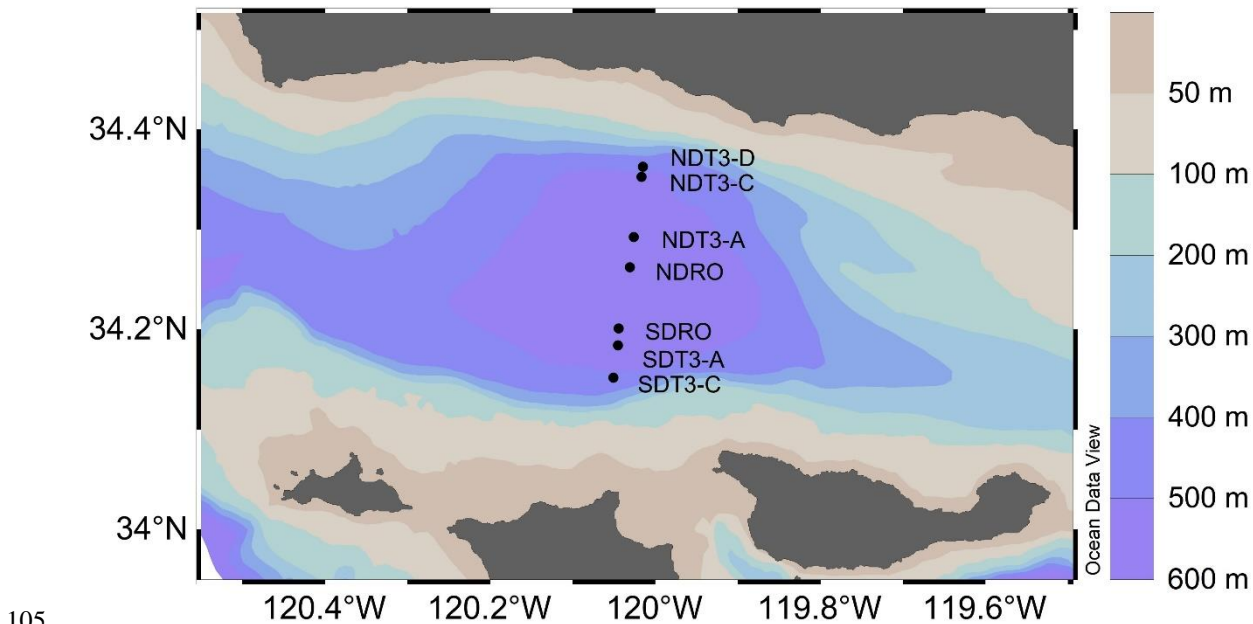


**Figure 1.** Sampling stations in the Santa Barbara Basin. The colour contours show bathymetry data from the General Bathymetric Chart of the Oceans at 30 arc seconds resolution (Becker et al., 2009) visualized in Ocean Data View v5.6.2 (Schlitzer, 2002).

110 **Table 1.** Sampling date, latitude, longitude, depth, bottom water concentrations of oxygen and nitrate, chamber  
 volume, total organic carbon (TOC) and nitrogen (TON), and C:N molar ratio of organic matter in the top 2 cm  
 of the sediment (by dry weight %) at the seven sampling stations in the Santa Barbara Basin. Oxygen  
 concentrations below detection limit of the Type 4831 (Aanderaa Data Instruments AS, Bergen, NO) oxygen  
 optode sensor (3  $\mu\text{M}$ ) and the Winkler titration method (1  $\mu\text{M}$ ) is denoted by “bdl”. Note that oxygen  
 concentrations in the bottom water at NDRO and SDRO were confirmed to be zero through additional analytical  
 115 methods (see Yousavich et al. 2024).

Station	NDT3-D	NDT3-C	NDT3-A	NDRO	SDRO	SDT3-A	SDT3-C
Date	7 Nov 2019	6 Nov 2019	4 Nov 2019	4 Nov 2019	3 Nov 2019	2 Nov 2019	8 Nov 2019
Latitude	34.363°N	34.353°N	34.292°N	34.261°N	34.201°N	34.184°N	34.152°N
Longitude	120.015°W	120.016°W	120.026°W	120.031°W	120.045°W	120.047°W	120.050°W
Depth (m)	447	498	572	580	586	571	494
Chamber ID	BFC1	BFC1	BFC1	BFC3	BFC1	BFC1	BFC1
Chamber volume (L)	3.435	4.321	3.925	3.791	2.416	2.719	3.092
Bottom water O <sub>2</sub> ( $\mu\text{M}$ )	8.7	5.2	9.2	bdl	bdl	bdl	3.1
Chamber O <sub>2</sub> ( $\mu\text{M}$ ) at T <sub>0</sub>	8.0	6.0	7.5	3.5	3.0	2.5	6.5
Chamber O <sub>2</sub> ( $\mu\text{M}$ ) at T <sub>end</sub>	7.0	6.5	8.5	10.0	1.0	1.7	6.5
Bottom water nitrate ( $\mu\text{M}$ )	27.3	26.0	24.4	18.5	9.9	20.4	16.3
Sediment TOC (%)	4.1%	4.6%	5.9%	5.7%	6.2%	6.8%	5.3%
Sediment TON (%)	0.5%	0.5%	0.7%	0.7%	0.8%	0.9%	0.6%
Sediment C:N ratio	10.33	10.10	9.46	9.37	9.28	8.79	9.63

120 Sediment samples for total organic carbon (TOC) and total organic nitrogen (TON) analyses were  
 subsampled from push cores (polycarbonate, 30.5 cm length, 6.35 cm inner diameter) retrieved by ROV

Jason that were sectioned in 1-cm increments up to 10 cm followed by 2-cm increments below 10 cm (Yousavich et al., 2024). Wet sediments were dried for up to 48 hours at 50°C and treated with 6N HCl to dissolve carbonate minerals (Harris et al., 2001). Samples were then washed with ultrapure water and dried again at 50°C. An aliquot (~10-15 mg) was then packed into individual 8x5 mm pressed tin capsules  
125 and analyzed at the University of California Davis stable isotope facility using a PDZ Europa 20-20 isotope ratio mass spectrometer (Sercon Ltd., Cheshire, UK). TOC and TON were calculated based on the sample peak area corrected against a reference material (alfalfa flour). Molar concentrations, obtained from measured TOC and TON (in wt%) were used to calculate carbon-to-nitrogen (C:N) ratios.

130 The design of the BFCs has been described previously (Vonnahme et al., 2020). In brief, a stirred cylindrical polycarbonate chamber (inner diameter = 19 cm) equipped with conductivity and oxygen sensors in the lid (type 5860 and 4330, respectively, Aanderaa Data Instruments AS, Bergen, NO) was inserted into the sediment to enclose a sediment patch of 284 cm<sup>2</sup> together with 2.5 to 4.5 L of overlying water. The chambers were outfitted with a syringe sampler hosting one injection syringe and six sampling  
135 syringes to inject into and take samples from the overlying water at approximately 60-minute intervals. The injection syringe contained 200 µmol of <sup>15</sup>N-labeled potassium nitrate (Cambridge Isotopes) dissolved in 50 ml of deionized water. To minimize the introduction of O<sub>2</sub>, the <sup>15</sup>N-labeled potassium nitrate solution was purged by ultra-high purity helium at 5 ml min<sup>-1</sup> for 60 minutes prior to be loaded into the injection syringe. The post-injection decrease in salinity in the chamber (as detected by the  
140 conductivity sensor) was used to calculate the volume of the benthic flux chamber (Kononets et al., 2021). Depending on the chamber volume, the total concentration of NO<sub>3</sub><sup>-</sup> ranged between 50 and 100 µM at the beginning of in-situ incubations. This level of NO<sub>3</sub><sup>-</sup> amendment was intended to prevent its depletion before the end of incubations given the potentially high rates of NO<sub>3</sub><sup>-</sup> uptake estimated by a previous study (Valentine et al., 2016).

145

After recovery, water samples from the BFC were transferred to evacuated 12-ml vials (Exetainer®, Labco, Lampeter, UK) pre-filled with 0.1 ml of 7 M zinc chloride for preservation. Prior to analysis of the isotopic compositions of N<sub>2</sub> and N<sub>2</sub>O, 5 mL sample was replaced with ultra-high purity helium to

create a headspace. The concentration and  $\delta^{15}\text{N}$  of dissolved  $\text{N}_2$  and  $\text{N}_2\text{O}$  was determined using a Sercon  
150 CryoPrep gas concentration system interfaced to a Sercon 20-20 isotope-ratio mass spectrometer (IRMS)  
at the University of California Davis Stable Isotope Facility. The measurement precision was  $\pm 0.2\text{‰}$  for  
 $\delta^{15}\text{N}$ .

Water samples from the benthic flux chambers for analysis of  $^{15}\text{NH}_4^+$  were filtered through sterile 47-mm  
155 syringe filters ( $0.2\ \mu\text{m}$  pore size) and frozen immediately. The production of  $^{15}\text{NH}_4^+$  in seawater samples  
was measured using a method adapted from *Zhang et al.* (2007) and described previously (Peng et al.,  
2016). In brief,  $\text{NH}_4^+$  was first oxidized to  $\text{NO}_2^-$  using hypobromite ( $\text{BrO}^-$ ) and then reduced to  $\text{N}_2\text{O}$  using  
an acetic acid-azide working solution (McIlvin and Altabet, 2005; Zhang et al., 2007). The  $\delta^{15}\text{N}$  of the  
produced  $\text{N}_2\text{O}$  was determined using an Elementar Americas PrecisION continuous flow, multicollector,  
160 isotope-ratio mass spectrometer (CF-MC-IRMS) coupled to a custom-built automated gas extraction and  
preparation system similar to the system described in McIlvin and Casciotti (2011). Calibration and  
correction were performed as described in Zhang et al. (2007). The measurement precision was  $\pm 0.2\text{‰}$   
for  $\delta^{15}\text{N}$ .  $\text{NH}_4^+$  solutions ( $10\ \mu\text{M}$ ) from a mixture of 99%  $^{15}\text{NH}_4\text{Cl}$  (Cambridge Isotopes) and IAEA  
standard N1 ( $\delta^{15}\text{N} = 1.2\text{‰}$ ) with a final  $\delta^{15}\text{N}$  of 135‰, 676‰, 1,351‰, 5,404‰, and 10,806‰ were  
165 prepared and used as in-house reference standards. The IRMS measurements of these in-house reference  
standards scaled linearly ( $R^2 = 0.9996$ ) with their  $\delta^{15}\text{N}$  values.

## 2.2 Rate calculations and statistics

Production rates of  $^{29}\text{N}_2$ ,  $^{30}\text{N}_2$ ,  $^{15}\text{NH}_4^+$ , and total  $\text{N}_2\text{O}$  were calculated from the slope of the concentrations  
of the respective species at the syringe sampling time points by fitting a linear regression multiplied by  
170 the overlying water column volume and divided by the chamber area. The linear regressions excluded the  
last one or two sampling time points if they clearly deviated from a linear trend compared to the first four  
or five sampling time points. The rates of  $\text{N}_2$  production from denitrification and anammox were  
calculated following a previously described method (Thamdrup and Dalsgaard, 2002) with modifications  
to account for coupled DNRA-anammox (Peng et al., 2021). The calculation was set up with  
175 denitrification rate ( $R_{\text{DN}}$ ) and anammox rate ( $R_{\text{AMX}}$ ) as unknowns:



$$R_{DN} \cdot f_N^2 + R_{AMX} \cdot f_A \cdot f_N = P^{30} \quad (\text{Eqn. 1})$$

$$R_{DN} \cdot 2 \cdot f_N \cdot (1 - f_N) + R_{AMX} \cdot [f_A \cdot (1 - f_N) + (1 - f_A) \cdot f_N] = P^{29} \quad (\text{Eqn. 2})$$

where  $P^{29}$  and  $P^{30}$  are the respective production rates of  $^{29}\text{N}_2$  and  $^{30}\text{N}_2$  that were calculated from measured concentrations stated above,  $f_N$  is the fraction of  $^{15}\text{N}$  in the  $\text{NO}_3^-$  pool and  $f_A$  is the fraction of  $^{15}\text{N}$  in the  $\text{NH}_4^+$  pool. The solution for  $R_{DN}$  and  $R_{AMX}$  is:

$$R_{DN} = \frac{(f_A + f_N - 2 \cdot f_A \cdot f_N) \cdot P^{30} - f_A \cdot f_N \cdot P^{29}}{f_N^2 \cdot (f_N - f_A)} \quad (\text{Eqn. 3})$$

$$R_{AMX} = \frac{f_N \cdot P^{29} - 2 \cdot (1 - f_N) \cdot P^{30}}{f_N \cdot (f_N - f_A)} \quad (\text{Eqn. 4})$$

Errors calculated from the linear regression of  $^{29}\text{N}_2$  and  $^{30}\text{N}_2$  production rates were propagated to  $R_{DN}$  and  $R_{AMX}$  following established statistical methods (Deming, 1943). Detection limits of the calculated rates were estimated as double the standard deviation from linear regressions. Depending on the in-situ  $\text{NO}_3^-$  concentration, the detection limit for total  $\text{N}_2$  production from denitrification and anammox ranged between 0.04 and 0.17  $\text{mmol m}^{-2} \text{d}^{-1}$  and 0.04 and 0.24  $\text{mmol m}^{-2} \text{d}^{-1}$  (Table S1), respectively. The detection limit for  $\text{N}_2\text{O}$  production ranged between 1.1 and 5.6  $\mu\text{mol m}^{-2} \text{d}^{-1}$ . DNRA rates were calculated as the rates of increase in  $^{15}\text{NH}_4^+$  divided by  $f^{15}$ , where  $f^{15}$  is the fraction of  $^{15}\text{N}$  in the  $\text{NO}_3^-$  pool. Because part of the produced  $^{15}\text{NH}_4^+$  would be adsorbed to sediment minerals, the rates of  $^{15}\text{NH}_4^+$  production were further multiplied by a factor of two (De Brabandere et al., 2015; Laima, 1994). Depending on the in-situ  $\text{NH}_4^+$  concentration, the detection limit for total  $\text{NH}_4^+$  production rates ranged between 0.01 and 0.07  $\text{mmol m}^{-2} \text{d}^{-1}$  (Table S1).

### 3 Results and Discussion

#### 3.1 Interpretation of rate measurements from benthic flux chamber incubations

The use of benthic flux chambers to perform  $^{15}\text{NO}_3^-$  incubation experiments in situ offers multiple advantages over other techniques such as slurry or whole-core incubations, including minimal disturbance of the sediment, maintenance of in-situ pressure and temperature, and relatively large surface area which can account for spatial heterogeneity (Aller et al., 1998; Hall et al., 2007; Nielsen and Glud, 1996; Robertson et al., 2019). On the other hand, several limitations of using tracer incubations with benthic

flux chambers can lead to either underestimated or overestimated rates. First, the diffusion of added  $^{15}\text{NO}_3^-$  into sediments and the labeled  $^{15}\text{NO}_3^-$  reduction products out of sediments in this study was unlikely at steady state.  $^{15}\text{NO}_3^-$  added to the overlying water of the chambers diffuses into sediment porewater where  $\text{O}_2$  is depleted within the first few millimeters, sustaining benthic  $\text{NO}_3^-$  reduction. However, a share of the labeled N-compounds that are produced will diffuse to pore waters in deeper sediment layers and, hence, cannot be detected in samples taken from the overlying waters. This can lead to an underestimation of  $\text{NO}_3^-$  reduction rates.

Second, the addition of  $\text{NO}_3^-$  at concentrations that were 1.6 - 6.2 (median = 2.3) times as high as ambient concentrations could lead to overestimation of rates. The  $\text{NO}_3^-$  uptake rates calculated as the decrease in total  $\text{NO}_3^-$  concentration over time was 1.9 - 6.4 (median = 3.8) times higher as those measured in parallel chambers deployed at the same time without any added  $^{15}\text{NO}_3^-$  (Table S2; (Yousavich et al., 2024). While the diffusive loss of  $\text{NO}_3^-$  to the sediment porewater is expected to account for the stimulated  $\text{NO}_3^-$  uptake partially,  $\text{NO}_3^-$  addition also likely stimulated the rates of  $\text{NO}_3^-$  reduction and intracellular storage. However, it remains unclear whether the accelerated  $\text{NO}_3^-$  uptake is partitioned between intracellular storage and reduction in the same proportion as under unamended conditions, which would partially depend on the carrying capacity of  $\text{NO}_3^-$  storage vs. reduction.

Third, the slight increase in  $\text{O}_2$  concentration in benthic chambers could have affected the rates of dissimilatory  $\text{NO}_3^-$  reduction and lead to underestimates.  $\text{O}_2$  in bottom water (and, therefore, also in pore waters) was depleted (below detection of the Winkler titration method, 1  $\mu\text{M}$ ) at the deepest stations SDRO and NDRO (Table 1).  $\text{O}_2$  concentrations in the overlying water in most incubations were slightly increasing over the period of the incubation with an average rate of  $0.11 \pm 0.44 \mu\text{mol h}^{-1}$ . The increase is attributed to a release of  $\text{O}_2$  from the polycarbonate walls and lids of the chambers that were exposed to air until shortly before deployment. The net increase in  $\text{O}_2$  in the overlying water indicates that rates of  $\text{O}_2$  provision from the plastics were in most cases higher than the rates of  $\text{O}_2$  uptake by the enclosed sediment. A release of  $\text{O}_2$  from plastics has been reported by a previous study which showed rates of  $\text{O}_2$  provided from polycarbonate to  $\text{O}_2$ -poor waters were among the highest of all plastics tested (Stevens,

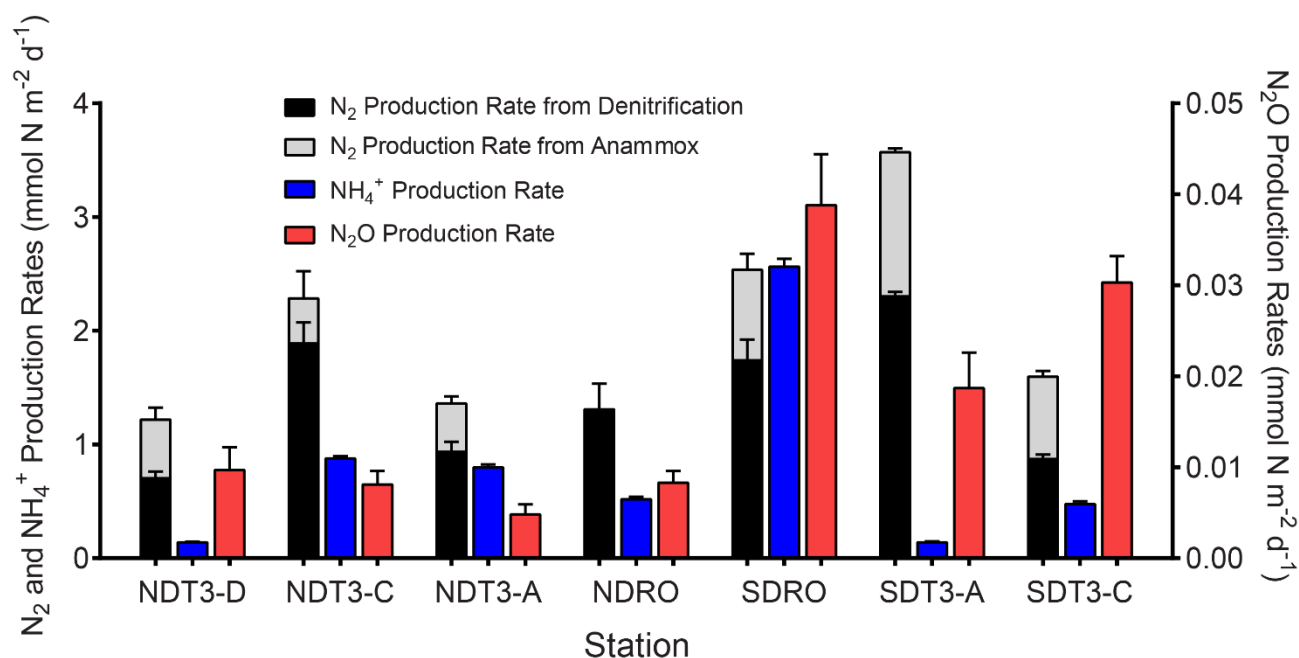
1992). The extent to which the artificial elevation of O<sub>2</sub> levels in the water overlaying the sediment in the chambers may have affected N-transformation pathways and rates will depend on the O<sub>2</sub> sensitivity of the respective processes and the penetration depth of O<sub>2</sub> into the sediment. This effect was likely insignificant in our incubations in the SBB because the rate of O<sub>2</sub> change was minimal compared to ambient O<sub>2</sub> concentrations except for station NDRO, where O<sub>2</sub> concentration in the chamber water rose from below detection to 10 μM (Table 1). While there are limitations that can lead to both underestimates and overestimates, there is the possibility that they level each other out and our observations are close to in situ production rates of N<sub>2</sub>, N<sub>2</sub>O, and NH<sub>4</sub><sup>+</sup>. Despite this concern, the relative contribution of different NO<sub>3</sub><sup>-</sup> reduction processes and the general trend of NO<sub>3</sub><sup>-</sup> reduction rates across the surveyed transect in the SBB are likely representative of in-situ conditions.

The NO<sub>3</sub><sup>-</sup> reduction rates measured in our experiments represent only the benthic contribution because the water samples in the six sampling syringes were sub-sampled simultaneously after recovery and no preservative was added inside the sampling syringe to terminate reactions. Therefore, we assume that NO<sub>3</sub><sup>-</sup> reduction in the overlying water (and in the syringes after respective samples have been taken) contributed equally among all six samples to the production of N<sub>2</sub>, N<sub>2</sub>O, and NH<sub>4</sub><sup>+</sup>, and does not interfere with our rate calculations. Separate water incubations would be needed to determine the rates of NO<sub>3</sub><sup>-</sup> reduction in the water column. To account for NH<sub>4</sub><sup>+</sup> adsorption which could lead to an underestimate of DNRA, we made the assumption that an amount of <sup>15</sup>NH<sub>4</sub><sup>+</sup> that equals the measured increase in the benthic flux chambers is adsorbed to sediment minerals (Hall et al., 2017; Laima, 1994). The rates determined in this study were determined during seasonal anoxia when bottom water O<sub>2</sub> was below detection at the depocenter of the basin. Additional expeditions are required to capture seasonal variations of these N cycling processes.

### **3.2 Denitrification was the dominant NO<sub>3</sub><sup>-</sup> reduction pathway**

On average, N<sub>2</sub> production by denitrification and anammox was dominant over DNRA in this study, accounting for 70.4 ± 16.4% of total NO<sub>3</sub><sup>-</sup> reduction (Fig. 2 and Table 2). Total N<sub>2</sub> production rates ranged

from 0.89 to 3.60 mmol N m<sup>-2</sup> d<sup>-1</sup>, which were lower compared to a previous estimate (~4.5 mmol N m<sup>-2</sup> d<sup>-1</sup>) based on NO<sub>3</sub><sup>-</sup> stable isotope mass balance calculations for the SBB (Sigman et al., 2003). Nevertheless, the previous estimate includes large uncertainties and the rates calculated from stable isotope mass balance represent signals integrated over multiple seasons (Sigman et al., 2003), whereas our measurements represent snapshots obtained in one season of one year when the bottom water NO<sub>3</sub><sup>-</sup> was not depleted. N<sub>2</sub> production rates at seasons more depleted in NO<sub>3</sub><sup>-</sup> concentrations in the bottom water compared to our study might more closely resemble rates estimated by Sigman et al. (2003). Season-resolving studies are needed in the future to understand the natural variability of the system and assess potential effects of stressors such as deoxygenation and rising temperature.



265

**Figure 2.** Inorganic N-species production rates determined from <sup>15</sup>N-NO<sub>3</sub><sup>-</sup> labelling studies with in-situ benthic flux chambers: Production of total N<sub>2</sub>, N<sub>2</sub> from denitrification, N<sub>2</sub> from anaerobic ammonia oxidation (anammox), NH<sub>4</sub><sup>+</sup> from dissimilatory nitrate reduction to ammonia (DNRA), and N<sub>2</sub>O. Note the lower range (right y-axis) for N<sub>2</sub>O production. Error bars represent standard errors of the calculated slope from linear regressions of N<sub>2</sub>/N<sub>2</sub>O production over time.

270

N<sub>2</sub> production rates in this study were higher than most of those reported in other studies using in-situ incubations with benthic flux chambers (Bonaglia et al., 2017; De Brabandere et al., 2015; Hall et al.,

2017; van Helmond et al., 2020; Hylén et al., 2022). Elevated rates in the SBB are likely a result of the  
275 high organic matter content of sediment (4.1 - 6.8% total organic carbon; Table 1), supporting high  
microbial respiration rates, and little (max. 20 mm) to zero O<sub>2</sub> penetration into the sediment (Yousavich  
et al., 2024). Compared to the SBB, organic matter content in sediment of previous studies, including the  
anoxic Eastern Gotland Basin (Hall et al., 2017), the largely pristine and oxygenated Gulf of Bothnia  
(Bonaglia et al., 2017), and an anoxic fjord basin in the By Fjord on the Swedish west coast (De  
280 Brabandere et al., 2015), was lower and the N<sub>2</sub> production rates were typically < 1 mmol N m<sup>-2</sup> d<sup>-1</sup>. In  
comparison, N<sub>2</sub> production rates reached 1.72 ± 0.77 mmol N m<sup>-2</sup> d<sup>-1</sup> in the sediment underlying eutrophic  
waters of Stockholm archipelago, where organic matter content was similar to SBB sediment (6.3% w/w)  
and O<sub>2</sub> penetration depth was < 4 mm (van Helmond et al., 2020). Additionally, benthic denitrification  
rates in the SBB (1.37 ± 0.64 mmol N m<sup>-2</sup> d<sup>-1</sup>) were similar to those reported from the Peruvian OMZ  
285 (1.31 ± 0.60 mmol N m<sup>-2</sup> d<sup>-1</sup>) where bottom water O<sub>2</sub> was lower than 10 μM and the organic matter content  
was similar (up to 7.5% TOC and 0.9% TON) to that in SBB sediments (Bohlen et al., 2011; Henrichs  
and Farrington, 1984; Sommer et al., 2016).

290 **Table 2.** The relative contribution of different processes (total N<sub>2</sub> production, N<sub>2</sub> from denitrification, N<sub>2</sub> from anammox, NH<sub>4</sub><sup>+</sup> from DNRA, and N<sub>2</sub>O Production) to total NO<sub>3</sub><sup>-</sup> reduction (upper part) and the relative contribution of total NO<sub>3</sub><sup>-</sup> reduction to total NO<sub>3</sub><sup>-</sup> uptake (lower part) in the Santa Barbara Basin. Total N<sub>2</sub> production consists of N<sub>2</sub> from denitrification and N<sub>2</sub> from anammox. Total NO<sub>3</sub><sup>-</sup> reduction consists of total N<sub>2</sub> production, NH<sub>4</sub><sup>+</sup> from DNRA, and N<sub>2</sub>O Production. Total NO<sub>3</sub><sup>-</sup> uptake consists of total NO<sub>3</sub><sup>-</sup> reduction and other NO<sub>3</sub><sup>-</sup> sinks (e.g. intracellular storage).

295

<b>Processes contributing to Total NO<sub>3</sub><sup>-</sup> Reduction</b>	<b>NDT3-D</b>	<b>NDT3-C</b>	<b>NDT3-A</b>	<b>NDRO</b>	<b>SDRO</b>	<b>SDT3-A</b>	<b>SDT3-C</b>
Total N <sub>2</sub> Production	85.8%	70.2%	59.2%	66.7%	45.1%	94.9%	71.1%
N <sub>2</sub> from Denitrification	59.2%	60.4%	49.3%	66.7%	38.3%	75.8%	56.8%
N <sub>2</sub> from Anammox	26.6%	9.8%	9.9%	0.0%	6.8%	19.1%	14.3%
NH <sub>4</sub> <sup>+</sup> from DNRA	13.3%	29.5%	40.6%	32.7%	54.1%	4.5%	27.3%
N <sub>2</sub> O Production	0.9%	0.3%	0.2%	0.6%	0.8%	0.6%	1.5%
<i>Total NO<sub>3</sub><sup>-</sup> Reduction</i>	100%	100%	100%	100%	100%	100%	100%
<b>Processes contributing to Total NO<sub>3</sub><sup>-</sup> Uptake</b>							
Total NO <sub>3</sub> <sup>-</sup> Reduction	7.4%	34.5%	16.3%	17.7%	57.7%	16.4%	17.5%
Other NO <sub>3</sub> <sup>-</sup> Sinks	92.6%	65.5%	83.7%	82.3%	42.3%	83.6%	82.5%
<i>Total NO<sub>3</sub><sup>-</sup> uptake</i>	100%	100%	100%	100%	100%	100%	100%

Benthic denitrification rates exceeded anammox rates at all sampling sites (Fig. 2 and Table 2). This relationship agrees with the paradigm that denitrification is typically favored over anammox in organic-rich sediments (Dalsgaard et al., 2005; Devol, 2015). Anammox bacteria can reduce NO<sub>3</sub><sup>-</sup> to NO<sub>2</sub><sup>-</sup>, which is then used to oxidize ammonia (NH<sub>3</sub>) to N<sub>2</sub> (Kartal et al., 2007). In our in-situ incubations, coupled DNRA-anammox in which DNRA produces a substrate (NH<sub>3</sub>) required by anammox could result in the production of <sup>30</sup>N<sub>2</sub> (Prokopenko et al., 2006), which is accounted for by our rate calculation method (detailed in section 2.2). However, because the porewater NH<sub>4</sub><sup>+</sup> concentration was high (> 100 μM) (Yousavich et al., 2024), the fraction of <sup>15</sup>N in the NH<sub>4</sub><sup>+</sup> pool remained low (up to 2.1% after ~1 hour of incubation and up to 4.3% after 6 hours of incubation). Therefore, the contribution of anammox to <sup>30</sup>N<sub>2</sub>

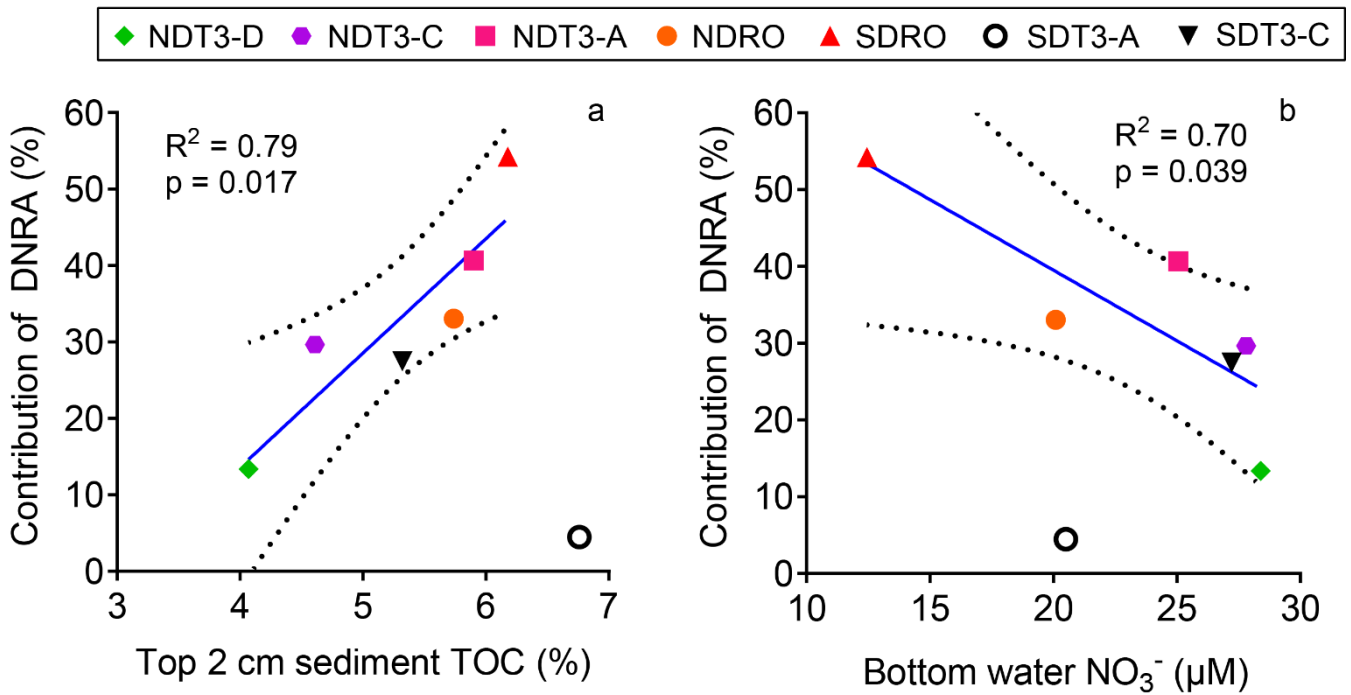
300

305

production was below 2.0% (Table S3). Overall, anammox contributed up to 26.6% of  $\text{NO}_3^-$  reduction in the SBB (Table 2), indicating that anammox was a significant process in benthic SBB N cycling. Because the N isotope fractionation during the reduction of nitrite ( $\text{NO}_2^-$ ) to  $\text{N}_2$  by anammox bacteria ( $+16.0 \pm 4.5\%$ ) is lower than that of denitrification used for isotope mass balance calculations ( $\sim 25\%$ ), anammox likely contributed to the lower-than-expected natural abundance  $^{15}\text{N}$  enrichment in the SBB water column  $\text{NO}_3^-$  pool previously measured (Brunner et al., 2013; Sigman et al., 2003). When  $\text{NO}_3^-$  is not limiting, denitrification typically dominates as the denitrifier population has a shorter generation time than DNRA bacteria (Kraft et al., 2014).

### 3.3 $\text{NO}_3^-$ availability and TOC control the relative importance of DNRA

The contribution of DNRA to total  $\text{NO}_3^-$  reduction was lower than denitrification at all stations except for the deepest station SDRO (Fig. 2), where  $\text{NH}_4^+$  production by DNRA contributed more than half of the  $\text{NO}_3^-$  reduction (Table 2). The relative contribution of DNRA to total  $\text{NO}_3^-$  reduction was positively correlated with TOC in the top 2 cm of the sediment (Fig. 3a) and negatively correlated with bottom water  $\text{NO}_3^-$  concentration (Fig. 3b). These trends are consistent with previous findings showing that DNRA tends to be favored in environments with high availability of electron donors such as organic carbon (Hardison et al., 2015; Kraft et al., 2014; Tiedje et al., 1983) and limited by  $\text{NO}_3^-$  (van den Berg et al., 2015; Kessler et al., 2018; Peng et al., 2016). Another example where DNRA dominated under limited  $\text{NO}_3^-$  availability is reported from measurements along a bottom water  $\text{O}_2$  and  $\text{NO}_3^-$  gradient traversing the Peruvian OMZ (Bohlen et al., 2011). One explanation for the increasing importance of DNRA under  $\text{NO}_3^-$ -limited conditions is that the growth yields calculated per mol electron acceptor from DNRA (consumes eight electrons) is higher than from denitrification (consumes five electrons) despite the greater amount of free energy provided by denitrification than DNRA per mol of  $\text{NO}_3^-$ , which was demonstrated by bacterial cultures capable of denitrification and DNRA (Strohm et al., 2007).



330

**Figure 3.** The correlation between the contribution of DNRA to  $\text{NO}_3^-$  reduction (in %) and (a) the C:N ratio of sediment organic matter and (b) the bottom water  $\text{NO}_3^-$  concentration in the Santa Barbara Basin. Linear regressions were performed excluding one outlier from station SDT3-A. The solid line represents the best fit, and the dashed lines represent the 95% confidence interval band.

335

The regressions we performed between the relative importance of DNRA vs. TOC and bottom water  $\text{NO}_3^-$  concentration excluded one data point from the station SDT3-A that deviated from the overall trend (Fig. 3). The DNRA rate at SDT3-A ( $0.14 \pm 0.005 \text{ mmol N m}^{-2} \text{ d}^{-1}$ ) was similarly low compared to NDT3-D ( $0.14 \pm 0.003 \text{ mmol N m}^{-2} \text{ d}^{-1}$ ), but the  $\text{N}_2$  production rates by both denitrification and anammox were the highest among all stations (Fig. 2), resulting in the lowest relative importance of DNRA. Porewater sulfide concentration was high at SDT3-A (Yousavich et al., 2024), so the DNRA bacteria should not be limited by the availability of electron donors. Sediments at SDT3-A were characterized by the highest TOC and TON content among all sites (Table 1), which may have fueled the highest rates of denitrification and anammox (Middelburg et al., 1996; Devol, 2015).

345



The frequency and magnitude of seasonal anoxia in the SBB has been increasing in the past four decades, which is expected to intensify fixed N loss and  $\text{NO}_3^-$  deficit in the water column (Goericke et al., 2015). Time-series measurements of water column  $\text{NO}_3^-$  revealed that bottom water  $\text{NO}_3^-$  depletion has become  
350 more frequent since 2003 compared to the time between 1986 and 2003. While seasonal flushing of the SBB not only oxygenates the bottom water but also increases bottom water  $\text{NO}_3^-$ , our results suggest that fixed N retention via DNRA will increase in response to  $\text{NO}_3^-$  drawdown even before  $\text{NO}_3^-$  is near depletion, which effectively forms negative feedback that could potentially prevent the depletion of fixed N in the SBB. On the other hand, when  $\text{NO}_3^-$  is no longer limiting, perhaps due to slowdown of bottom  
355 water deoxygenation, the relative importance of DNRA would decrease, allowing denitrification to dominate  $\text{NO}_3^-$  reduction pathways.

### 3.4 $\text{N}_2\text{O}$ production and saturation

$\text{N}_2\text{O}$  production rates measured by in-situ chamber incubations ranged from  $4.8 \pm 1.1$  to  $38.8 \pm 5.6$   $\mu\text{mol m}^{-2} \text{d}^{-1}$  (Fig. 2). These rates were up to an order of magnitude higher than those measured using shipboard  
360 whole-core incubations ( $3.5 \pm 1.0$   $\mu\text{mol m}^{-2} \text{d}^{-1}$ ) with samples from a similar depth (544 m) in the anoxic part of the Soledad Basin (Townsend-Small et al., 2014). A recent study using in-situ chamber incubations with  $^{15}\text{NO}_3^-$  in the Eastern Gotland Basin reported rates ( $\sim 15 - 68$   $\mu\text{mol m}^{-2} \text{d}^{-1}$ ) similar to or higher than the rates we measured in the SBB (Hylén et al., 2022). Because the physicochemical context of the Soledad Basin is more similar to the SBB than the Eastern Gotland Basin, we expected the  $\text{N}_2\text{O}$   
365 production rates in the Soledad Basin to be close to those in the SBB. The much lower  $\text{N}_2\text{O}$  production rates reported from the Soledad Basin may be partially attributed to the whole-core incubations that were not performed in situ.

$\text{N}_2\text{O}$  production as a fraction of total  $\text{NO}_3^-$  reduction ranged from 0.2% to 1.5% (Table 2), which fell in  
370 the typical range of  $\text{N}_2\text{O}$  yield from both nitrification and denitrification (Ji et al., 2015, 2018). Although our measurements do not allow the distinction between  $\text{N}_2\text{O}$  production from nitrification and denitrification, it is likely that both processes contributed with the respective share depending on ambient  $\text{O}_2$  concentration. At the deepest stations where bottom water  $\text{O}_2$  was depleted (Table 1), denitrification

was likely the main source of N<sub>2</sub>O. At other stations, where bottom water O<sub>2</sub> ranged from 3.1 - 9.2 μM, nitrification likely also contributed to N<sub>2</sub>O production.

Although we observed N<sub>2</sub>O production in all in-situ <sup>15</sup>NO<sub>3</sub><sup>-</sup> incubations, N<sub>2</sub>O concentration in the chambers at the start of the incubations was far below saturation level (9 - 12%) at the two deepest stations SDRO and NDRO (Table S4). In contrast, N<sub>2</sub>O was either close to or above saturation at all other stations (Table S4). The low concentration of dissolved N<sub>2</sub>O at the two deepest stations is consistent with our finding that N<sub>2</sub> production (i.e., N<sub>2</sub>O consumption) rates by denitrification were the highest there (Fig. 2), indicating that the deepest part of the SBB typically acts as a sink for N<sub>2</sub>O. The shallower parts of the SBB were characterized by a lower NO<sub>3</sub><sup>-</sup> uptake rate (Table S2; Fig. S1), but they had a stronger potential for N<sub>2</sub>O production than the deepest stations (Fig. S2). In case of a eutrophication event, enhanced surface primary productivity could stimulate denitrification as well as N<sub>2</sub>O production in the shallower parts of the SBB where bottom water O<sub>2</sub> is not depleted, where benthic N<sub>2</sub>O production is more likely to contribute to N<sub>2</sub>O efflux from the water column during upwelling events.

### **3.5 Total NO<sub>3</sub><sup>-</sup> uptake suggests high potential for intracellular NO<sub>3</sub><sup>-</sup> storage**

Although the N<sub>2</sub> production rates we measured in the SBB were among the highest reported values for any marine sediments, total NO<sub>3</sub><sup>-</sup> reduction, which also includes DNRA and N<sub>2</sub>O production, only accounted for 23.9 ± 16.9% of the total NO<sub>3</sub><sup>-</sup> uptake in benthic flux chambers amended with <sup>15</sup>NO<sub>3</sub><sup>-</sup> (Table 2). Intracellular NO<sub>3</sub><sup>-</sup> storage by bacteria and microbial eukaryotes was likely responsible for the majority of the NO<sub>3</sub><sup>-</sup> uptake unaccounted for by the different NO<sub>3</sub><sup>-</sup> reduction pathways. Marine *Beggiatoa* spp. can hyper-accumulate NO<sub>3</sub><sup>-</sup> intracellularly at concentrations 3,000- to 4,000-fold above ambient levels (McHatton et al., 1996). Other microbial lineages including *Thioploca*, foraminifera, and gromiida are also known to store NO<sub>3</sub><sup>-</sup> intracellularly (Piña-Ochoa et al., 2010; Zopfi et al., 2001). In two of the porewater profiles sampled during the same cruise, NO<sub>3</sub><sup>-</sup> concentrations at 1 cm depth reached 80 - 390 μM, which we interpreted as evidence of NO<sub>3</sub><sup>-</sup> leakage from bacterial cells during porewater handling (Yousavich et al., 2024). While it is difficult to directly constrain the contribution of intracellular NO<sub>3</sub><sup>-</sup> storage to total NO<sub>3</sub><sup>-</sup> uptake, it can be indirectly inferred by calculating the diffusive loss (both upward

and downward) of added  $^{15}\text{NO}_3^-$  if porewater concentrations in sediments underlying the benthic flux chamber were available.

The total  $\text{NO}_3^-$  uptake in the SBB measured from parallel benthic flux chambers without substrate amendment at the same stations ( $3.26 \pm 0.72 \text{ mmol N m}^{-2} \text{ d}^{-1}$ ) (Yousavich et al., 2024) was higher than that in other nearby borderland basins such as the San Nicolas Basin ( $0.38 \pm 0.03 \text{ mmol N m}^{-2} \text{ d}^{-1}$ ), the San Pedro Basin ( $0.78 \pm 0.11 \text{ mmol N m}^{-2} \text{ d}^{-1}$ ) (Berelson et al., 1987), and the Santa Monica Basin ( $1.10 \pm 0.31 \text{ mmol N m}^{-2} \text{ d}^{-1}$ ) (Jahnke, 1990). As mentioned above (section 3.1), the addition of  $^{15}\text{NO}_3^-$  stimulated  $\text{NO}_3^-$  uptake rates by multiple folds (compared to BFC incubations without  $^{15}\text{NO}_3^-$  additions) and to a level ( $11.60 \pm 4.15 \text{ mmol N m}^{-2} \text{ d}^{-1}$ ) similar to a previous estimate ( $11.7 \text{ mmol N m}^{-2} \text{ d}^{-1}$ ) based on water column  $\text{NO}_3^-$  deficit (Valentine et al., 2016). Since bottom water  $\text{NO}_3^-$  during our sampling time ( $>12.5 \mu\text{M}$  in November 2019) was not as depleted as in October 2013 ( $\sim 2 \mu\text{M NO}_3^-$ ) (Valentine et al., 2016), these results indicate that the microbial community in SBB sediments have the metabolic potential to further consume  $\text{NO}_3^-$  when SBB bottom water undergoes extended periods (months) of anoxia during autumn and winter. Assuming that  $\text{NO}_3^-$  in the lowermost 10 m of the water column are under direct influence of benthic  $\text{NO}_3^-$  uptake, we estimate it would take between one to four months to deplete bottom water  $\text{NO}_3^-$  with a starting concentration of  $30 \mu\text{M}$ , with the shortest depletion time at the depocenter and the longest at the periphery of the SBB. This timescale agrees with time-series measurements of water-column  $\text{NO}_3^-$  concentrations in the SBB (Goericke et al., 2015), and it implies that bottom water  $\text{NO}_3^-$  is unlikely to become depleted at depths shallower than 500 m. Furthermore, we identified a significant negative correlation between  $\text{NO}_3^-$  uptake rates without substrate amendments and the fold-change after  $^{15}\text{NO}_3^-$  addition (Fig. S3). This negative correlation indicates that benthic  $\text{NO}_3^-$  uptake rates at the shallow stations were the most responsive to exogenous  $\text{NO}_3^-$  supply, while on the other hand  $\text{NO}_3^-$  uptake rates at the deep and anoxic stations were closer to an upper limit that is determined by the microbial community present in the SBB sediments.

## 4 Summary

We investigated benthic nitrogen cycling processes using in-situ incubations with  $^{15}\text{NO}_3^-$  addition and quantified the rates of total  $\text{NO}_3^-$  uptake, denitrification, anammox,  $\text{N}_2\text{O}$  production, and DNRA. Our results indicate the role of the SBB sediments as a strong sink for fixed N. Denitrification was the dominant  $\text{NO}_3^-$  reduction process (38-76%), while anammox contributed up to 27%. DNRA accounted for less than half of  $\text{NO}_3^-$  reduction except at the deepest station (586 m), at the center of the SBB, where bottom water  $\text{O}_2$  concentrations were zero. The elevated relative importance of DNRA under high TOC and low  $\text{NO}_3^-$  conditions suggests that the fixed N loss in the SBB, especially during seasons of high surface primary productivity and thus high export production, could potentially be balanced by the N retention pathway. The higher  $\text{N}_2\text{O}$  production measured in this study compared to nearby borderland basins may have stemmed from the use of benthic chambers instead of whole-core incubations, which highlights the advantage of in-situ incubations in determining benthic N cycling processes. The high potential and relative importance of intracellular  $\text{NO}_3^-$  storage implied by our data poses a challenge to fully constrain the fixed N budget in the SBB, but it also presents an opportunity for future investigations targeting intracellular storage. Future intensification of water column anoxia may elevate the importance of fixed N retention via DNRA by keeping N in the system as  $\text{NH}_4^+$ , forming negative feedback that could overall reduce fixed N loss in the SBB.

### Data availability

The rate data in tabular form are available at [https://figshare.com/articles/dataset/Peng\\_et\\_al\\_2023\\_xlsx/21824610](https://figshare.com/articles/dataset/Peng_et_al_2023_xlsx/21824610).

### Author contribution

XP, TT, and DLV designed the study; XP, DJY, FW, FJ, TT, and DLV participated in the fieldwork; XP, DJY, AB, FW, and FJ performed the measurements; XP wrote the manuscript; All authors contributed to the writing of the manuscript and discussion of the data.

## **Competing interests**

One of the co-authors is a member of the editorial board of Biogeosciences.

## **Acknowledgements**

455 We thank the captain, crew, and scientific party of the R/V Atlantis, and the crew of the ROV Jason for their technical and logistical support during the research expedition AT42-19. We also thank D. Robinson, S. Krause, Q. Qin, E. Arrington, M. O'Beirne, A. Mazariegos, X. Moreno, A. Eastman, H. Kittner, S. Dorji, J. Burgos-Ponce, N. Liu, J. Tarn, and K. Gosselin for assisting with shipboard analyses. Funding for this work was provided by the US National Science Foundation, NSF OCE-1756947 and OCE-1830033 (to DLV) and OCE-1829981 (to TT), and by a Simons Foundation Postdoctoral Fellowship in  
460 Marine Microbial Ecology (No. 547606 to XP). F Wenzhöfer was partly funded through the Danish National Research Foundation (DNRF145 - HADAL).

465 **References**

- Aller, R. C., Hall, P. O. J., Rude, P. D., and Aller, J. Y.: Biogeochemical heterogeneity and suboxic diagenesis in hemipelagic sediments of the Panama Basin, *Deep Sea Research Part I: Oceanographic Research Papers*, 45, 133–165, [https://doi.org/10.1016/S0967-0637\(97\)00049-6](https://doi.org/10.1016/S0967-0637(97)00049-6), 1998.
- 470 Becker, J. J., Sandwell, D. T., Smith, W. H. F., Braud, J., Binder, B., Depner, J., Fabre, D., Factor, J., Ingalls, S., Kim, S.-H., Ladner, R., Marks, K., Nelson, S., Pharaoh, A., Trimmer, R., Von Rosenberg, J., Wallace, G., and Weatherall, P.: Global Bathymetry and Elevation Data at 30 Arc Seconds Resolution: SRTM30\_PLUS, *Marine Geodesy*, 32, 355–371, <https://doi.org/10.1080/01490410903297766>, 2009.
- 475 Berelson, W. M., Hammond, D. E., and Johnson, K. S.: Benthic fluxes and the cycling of biogenic silica and carbon in two southern California borderland basins, *Geochimica et Cosmochimica Acta*, 51, 1345–1363, [https://doi.org/10.1016/0016-7037\(87\)90320-6](https://doi.org/10.1016/0016-7037(87)90320-6), 1987.
- van den Berg, E. M., van Dongen, U., Abbas, B., and van Loosdrecht, M. C.: Enrichment of DNRA bacteria in a continuous culture, *ISME J*, 9, 2153–2161, <https://doi.org/10.1038/ismej.2015.26>, 2015.
- 480 Bernhard, J. M., Casciotti, K. L., McIlvin, M. R., Beaudoin, D. J., Visscher, P. T., and Edgcomb, V. P.: Potential importance of physiologically diverse benthic foraminifera in sedimentary nitrate storage and respiration, *Journal of Geophysical Research: Biogeosciences*, 117, <https://doi.org/10.1029/2012JG001949>, 2012.
- Bograd, S. J., Schwing, F. B., Castro, C. G., and Timothy, D. A.: Bottom water renewal in the Santa Barbara Basin, *Journal of Geophysical Research: Oceans*, 107, 9-1-9–9, <https://doi.org/10.1029/2001JC001291>, 2002.
- 485 Bohlen, L., Dale, A. W., Sommer, S., Mosch, T., Hensen, C., Noffke, A., Scholz, F., and Wallmann, K.: Benthic nitrogen cycling traversing the Peruvian oxygen minimum zone, *Geochimica et Cosmochimica Acta*, 75, 6094–6111, <https://doi.org/10.1016/j.gca.2011.08.010>, 2011.
- Bonaglia, S., Hylén, A., Rattray, J. E., Kononets, M. Y., Ekeröth, N., Roos, P., Thamdrup, B., Brüchert, V., and Hall, P. O. J.: The fate of fixed nitrogen in marine sediments with low organic loading: an in situ study, *Biogeosciences*, 14, 285–300, <https://doi.org/10.5194/bg-14-285-2017>, 2017.
- 490 Brunner, B., Contreras, S., Lehmann, M. F., Matantseva, O., Rollog, M., Kalvelage, T., Klockgether, G., Lavik, G., Jetten, M. S. M., Kartal, B., and Kuypers, M. M. M.: Nitrogen isotope effects induced by anammox bacteria, *Proceedings of the National Academy of Sciences*, 110, 18994–18999, <https://doi.org/10.1073/pnas.1310488110>, 2013.
- Burgin, A. J. and Hamilton, S. K.: Have we overemphasized the role of denitrification in aquatic ecosystems? A review of nitrate removal pathways, *Frontiers in Ecology and the Environment*, 5, 89–96, [https://doi.org/10.1890/1540-9295\(2007\)5\[89:HWOTRO\]2.0.CO;2](https://doi.org/10.1890/1540-9295(2007)5[89:HWOTRO]2.0.CO;2), 2007.
- 495 Caffrey, J. M., Bonaglia, S., and Conley, D. J.: Short exposure to oxygen and sulfide alter nitrification, denitrification, and DNRA activity in seasonally hypoxic estuarine sediments, *FEMS Microbiology Letters*, 366, fny288, <https://doi.org/10.1093/femsle/fny288>, 2019.
- Dalsgaard, T., Thamdrup, B., and Canfield, D. E.: Anaerobic ammonium oxidation (anammox) in the marine environment, *Research in Microbiology*, 156, 457–464, <https://doi.org/10.1016/j.resmic.2005.01.011>, 2005.

- 500 Dalsgaard, T., Stewart, F. J., Thamdrup, B., Brabandere, L. D., Revsbech, N. P., Ulloa, O., Canfield, D. E., and DeLong, E. F.: Oxygen at Nanomolar Levels Reversibly Suppresses Process Rates and Gene Expression in Anammox and Denitrification in the Oxygen Minimum Zone off Northern Chile, *mBio*, 5, <https://doi.org/10.1128/mBio.01966-14>, 2014.
- De Brabandere, L., Bonaglia, S., Kononets, M. Y., Viktorsson, L., Stigebrandt, A., Thamdrup, B., and Hall, P. O. J.: Oxygenation of an anoxic fjord basin strongly stimulates benthic denitrification and DNRA, *Biogeochemistry*, 126, 131–152, 505 <https://doi.org/10.1007/s10533-015-0148-6>, 2015.
- Deming, W. E.: *Statistical adjustment of data.*, 1943.
- Devol, A. H.: Denitrification, Anammox, and N<sub>2</sub> Production in Marine Sediments, *Annual Review of Marine Science*, 7, 403–423, <https://doi.org/10.1146/annurev-marine-010213-135040>, 2015.
- Elkins, J. W., Wofsy, S. C., McElroy, M. B., Kolb, C. E., and Kaplan, W. A.: Aquatic sources and sinks for nitrous oxide, 510 *Nature*, 275, 602–606, <https://doi.org/10.1038/275602a0>, 1978.
- Firestone, M. K., Firestone, R. B., and Tiedje, J. M.: Nitrous Oxide from Soil Denitrification: Factors Controlling Its Biological Production, *Science*, 208, 749–751, <https://doi.org/10.1126/science.208.4445.749>, 1980.
- García-Robledo, E., Corzo, A., and Pappaspyrou, S.: A fast and direct spectrophotometric method for the sequential determination of nitrate and nitrite at low concentrations in small volumes, *Marine Chemistry*, 162, 30–36, 515 <https://doi.org/10.1016/j.marchem.2014.03.002>, 2014.
- Goericke, R., Bograd, S. J., and Grundle, D. S.: Denitrification and flushing of the Santa Barbara Basin bottom waters, *Deep Sea Research Part II: Topical Studies in Oceanography*, 112, 53–60, <https://doi.org/10.1016/j.dsr2.2014.07.012>, 2015.
- Gruber, N.: The marine nitrogen cycle: overview and challenges, *Nitrogen in the marine environment*, 2, 1–50, 2008.
- Hall, P. O. J., Brunnegård, J., Hulthe, G., Martin, W. R., Stahl, H., and Tengberg, A.: Dissolved organic matter in abyssal sediments: Core recovery artifacts, *Limnology and Oceanography*, 52, 19–31, <https://doi.org/10.4319/lo.2007.52.1.0019>, 2007.
- Hall, P. O. J., Almroth Rosell, E., Bonaglia, S., Dale, A. W., Hylén, A., Kononets, M., Nilsson, M., Sommer, S., van de Velde, S., and Viktorsson, L.: Influence of Natural Oxygenation of Baltic Proper Deep Water on Benthic Recycling and Removal of Phosphorus, Nitrogen, Silicon and Carbon, *Front. Mar. Sci.*, 4, <https://doi.org/10.3389/fmars.2017.00027>, 2017.
- 525 Hardison, A. K., Algar, C. K., Giblin, A. E., and Rich, J. J.: Influence of organic carbon and nitrate loading on partitioning between dissimilatory nitrate reduction to ammonium (DNRA) and N<sub>2</sub> production, *Geochimica et Cosmochimica Acta*, 164, 146–160, <https://doi.org/10.1016/j.gca.2015.04.049>, 2015.
- Harris, D., Horwath, W. R., and van Kessel, C.: Acid fumigation of soils to remove carbonates prior to total organic carbon or CARBON-13 isotopic analysis, *Soil Science Society of America Journal*, 65, 1853–1856, 530 <https://doi.org/10.2136/sssaj2001.1853>, 2001.
- van Helmond, N. A. G. M., Robertson, E. K., Conley, D. J., Hermans, M., Humborg, C., Kubeneck, L. J., Lenstra, W. K., and Slomp, C. P.: Removal of phosphorus and nitrogen in sediments of the eutrophic Stockholm archipelago, Baltic Sea, *Biogeosciences*, 17, 2745–2766, <https://doi.org/10.5194/bg-17-2745-2020>, 2020.
- Henrichs, S. M. and Farrington, J. W.: Peru upwelling region sediments near 15°S. 1. Remineralization and accumulation of organic matter<sup>1</sup>, *Limnology and Oceanography*, 29, 1–19, <https://doi.org/10.4319/lo.1984.29.1.0001>, 1984.

- Horak, R. E. A., Ruef, W., Ward, B. B., and Devol, A. H.: Expansion of denitrification and anoxia in the eastern tropical North Pacific from 1972 to 2012, *Geophys. Res. Lett.*, 43, 2016GL068871, <https://doi.org/10.1002/2016GL068871>, 2016.
- 540 Hylén, A., Bonaglia, S., Robertson, E., Marzocchi, U., Kononets, M., and Hall, P. O. J.: Enhanced benthic nitrous oxide and ammonium production after natural oxygenation of long-term anoxic sediments, *Limnology and Oceanography*, 67, 419–433, <https://doi.org/10.1002/lno.12001>, 2022.
- Jahnke, R. A.: Early diagenesis and recycling of biogenic debris at the seafloor, Santa Monica Basin, California, *Journal of Marine Research*, 48, 413–436, <https://doi.org/10.1357/002224090784988773>, 1990.
- 545 Ji, Q., Babbin, A. R., Jayakumar, A., Oleynik, S., and Ward, B. B.: Nitrous oxide production by nitrification and denitrification in the Eastern Tropical South Pacific oxygen minimum zone, *Geophysical Research Letters*, 42, 10,755-10,764, <https://doi.org/10.1002/2015GL066853>, 2015.
- Ji, Q., Buitenhuis, E., Suntharalingam, P., Sarmiento, J. L., and Ward, B. B.: Global Nitrous Oxide Production Determined by Oxygen Sensitivity of Nitrification and Denitrification, *Global Biogeochemical Cycles*, 32, 1790–1802, <https://doi.org/10.1029/2018GB005887>, 2018.
- 550 Joye, S. B. and Hollibaugh, J. T.: Influence of Sulfide Inhibition of Nitrification on Nitrogen Regeneration in Sediments, *Science*, 270, 623–625, <https://doi.org/10.1126/science.270.5236.623>, 1995.
- Kamp, A., Høglund, S., Risgaard-Petersen, N., and Stief, P.: Nitrate Storage and Dissimilatory Nitrate Reduction by Eukaryotic Microbes, *Front. Microbiol.*, 6, <https://doi.org/10.3389/fmicb.2015.01492>, 2015.
- 555 Kartal, B., Kuypers, M. M. M., Lavik, G., Schalk, J., Op den Camp, H. J. M., Jetten, M. S. M., and Strous, M.: Anammox bacteria disguised as denitrifiers: nitrate reduction to dinitrogen gas via nitrite and ammonium, *Environmental Microbiology*, 9, 635–642, <https://doi.org/10.1111/j.1462-2920.2006.01183.x>, 2007.
- Kessler, A. J., Roberts, K. L., Bissett, A., and Cook, P. L. M.: Biogeochemical Controls on the Relative Importance of Denitrification and Dissimilatory Nitrate Reduction to Ammonium in Estuaries, *Global Biogeochemical Cycles*, 32, 1045–1057, <https://doi.org/10.1029/2018GB005908>, 2018.
- 560 Kononets, M., Tengberg, A., Nilsson, M., Ekeröth, N., Hylén, A., Robertson, E. K., van de Velde, S., Bonaglia, S., Rütting, T., Blomqvist, S., and Hall, P. O. J.: In situ incubations with the Gothenburg benthic chamber landers: Applications and quality control, *Journal of Marine Systems*, 214, 103475, <https://doi.org/10.1016/j.jmarsys.2020.103475>, 2021.
- Koslow, J., Goericke, R., McClatchie, S., Vetter, R., and Rogers-Bennett, L.: *The California Cooperative Oceanic Fisheries Investigations (CalCOFI): the continuing evolution and contributions of a 60-year ocean observation program*, 2010.
- 565 Kraft, B., Tegetmeyer, H. E., Sharma, R., Klotz, M. G., Ferdelman, T. G., Hettich, R. L., Geelhoed, J. S., and Strous, M.: The environmental controls that govern the end product of bacterial nitrate respiration, *Science*, 345, 676–679, <https://doi.org/10.1126/science.1254070>, 2014.
- Laima, M. C. J.: Is KCl a reliable extractant of  $15\text{NH}_4^+$  added to coastal marine sediments? *Biogeochemistry*, 27, 83–95, <https://doi.org/10.1007/BF00002812>, 1994.
- 570 McHatton, S. C., Barry, J. P., Jannasch, H. W., and Nelson, D. C.: High Nitrate Concentrations in Vacuolate, Autotrophic Marine Beggiatoa spp, *Applied and Environmental Microbiology*, 62, 954–958, <https://doi.org/10.1128/aem.62.3.954-958.1996>, 1996.



- McIlvin, M. R. and Altabet, M. A.: Chemical Conversion of Nitrate and Nitrite to Nitrous Oxide for Nitrogen and Oxygen Isotopic Analysis in Freshwater and Seawater, *Anal. Chem.*, 77, 5589–5595, <https://doi.org/10.1021/ac050528s>, 2005.
- 575 Middelburg, J. J., Soetaert, K., Herman, P. M. J., and Heip, C. H. R.: Denitrification in marine sediments: A model study, *Global Biogeochemical Cycles*, 10, 661–673, <https://doi.org/10.1029/96GB02562>, 1996.
- Myhre, S. E., Pak, D., Borreggine, M., Kennett, J. P., Nicholson, C., Hill, T. M., and Deutsch, C.: Oxygen minimum zone biotic baseline transects for paleoceanographic reconstructions in Santa Barbara Basin, CA, *Deep Sea Research Part II: Topical Studies in Oceanography*, 150, 118–131, <https://doi.org/10.1016/j.dsr2.2017.12.009>, 2018.
- 580 Nielsen, L. P. and Glud, R. N.: Denitrification in a coastal sediment measured in situ by the nitrogen isotope pairing technique applied to a benthic flux chamber, *Marine Ecology Progress Series*, 137, 181–186, <https://doi.org/10.3354/meps137181>, 1996.
- Oschlies, A., Duteil, O., Getzlaff, J., Koeve, W., Landolfi, A., and Schmidtko, S.: Patterns of deoxygenation: sensitivity to natural and anthropogenic drivers, *Philosophical Transactions of the Royal Society A: Mathematical, Physical and Engineering Sciences*, 375, 20160325, <https://doi.org/10.1098/rsta.2016.0325>, 2017.
- 585 Paulmier, A. and Ruiz-Pino, D.: Oxygen minimum zones (OMZs) in the modern ocean, *Progress in Oceanography*, 80, 113–128, <https://doi.org/10.1016/j.pocean.2008.08.001>, 2009.
- Peng, X., Ji, Q., Angell, J. H., Kearns, P. J., Yang, H. J., Bowen, J. L., and Ward, B. B.: Long-term fertilization alters the relative importance of nitrate reduction pathways in salt marsh sediments, *J. Geophys. Res. Biogeosci.*, 2016JG003484, <https://doi.org/10.1002/2016JG003484>, 2016.
- 590 Peng, X., Ji, Q., Angell, J. H., Kearns, P. J., Bowen, J. L., and Ward, B. B.: Long-Term Fertilization Alters Nitrous Oxide Cycling Dynamics in Salt Marsh Sediments, *Environ. Sci. Technol.*, 55, 10832–10842, <https://doi.org/10.1021/acs.est.1c01542>, 2021.
- Piña-Ochoa, E., Høgslund, S., Geslin, E., Cedhagen, T., Revsbech, N. P., Nielsen, L. P., Schweizer, M., Jorissen, F., Rysgaard, S., and Risgaard-Petersen, N.: Widespread occurrence of nitrate storage and denitrification among Foraminifera and Gromiida, *Proceedings of the National Academy of Sciences*, 107, 1148–1153, <https://doi.org/10.1073/pnas.0908440107>, 2010.
- 595 Prokopenko, M. G., Hammond, D. E., Berelson, W. M., Bernhard, J. M., Stott, L., and Douglas, R.: Nitrogen cycling in the sediments of Santa Barbara basin and Eastern Subtropical North Pacific: Nitrogen isotopes, diagenesis and possible chemosymbiosis between two lithotrophs (*Thioploca* and *Anammox*)—“riding on a glider,” *Earth and Planetary Science Letters*, 242, 186–204, <https://doi.org/10.1016/j.epsl.2005.11.044>, 2006.
- 600 Qin, Q., Kinnaman, F. S., Gosselin, K. M., Liu, N., Treude, T., and Valentine, D. L.: Seasonality of water column methane oxidation and deoxygenation in a dynamic marine environment, *Geochimica et Cosmochimica Acta*, 336, 219–230, <https://doi.org/10.1016/j.gca.2022.09.017>, 2022.
- Reimers, C. E., Lange, C. B., Tabak, M., and Bernhard, J. M.: Seasonal spillover and varve formation in the Santa Barbara Basin, California, *Limnology and Oceanography*, 35, 1577–1585, <https://doi.org/10.4319/lo.1990.35.7.1577>, 1990.
- 605 Robertson, E. K., Bartoli, M., Brüchert, V., Dalsgaard, T., Hall, P. O. J., Hellemann, D., Hietanen, S., Zilius, M., and Conley, D. J.: Application of the isotope pairing technique in sediments: Use, challenges, and new directions, *Limnology and Oceanography: Methods*, 17, 112–136, <https://doi.org/10.1002/lom3.10303>, 2019.
- Schlitzer, R.: Interactive analysis and visualization of geoscience data with Ocean Data View, *Computers & Geosciences*, 28, 1211–1218, [https://doi.org/10.1016/S0098-3004\(02\)00040-7](https://doi.org/10.1016/S0098-3004(02)00040-7), 2002.

- Schulz, H. N., Brinkhoff, T., Ferdelman, T. G., Mariné, M. H., Teske, A., and Jørgensen, B. B.: Dense Populations of a Giant Sulfur Bacterium in Namibian Shelf Sediments, *Science*, 284, 493–495, <https://doi.org/10.1126/science.284.5413.493>, 1999.
- Shao, M.-F., Zhang, T., Fang, H. H.-P., and Li, X.: The effect of nitrate concentration on sulfide-driven autotrophic denitrification in marine sediment, *Chemosphere*, 83, 1–6, <https://doi.org/10.1016/j.chemosphere.2011.01.042>, 2011.
- Sholkovitz, E. R. and Gieskes, J. M.: A Physical-Chemical Study of the Flushing of the Santa Barbara Basin1, *Limnology and Oceanography*, 16, 479–489, <https://doi.org/10.4319/lo.1971.16.3.0479>, 1971.
- 615 Sigman, D. M., Robinson, R., Knapp, A. N., van Geen, A., McCorkle, D. C., Brandes, J. A., and Thunell, R. C.: Distinguishing between water column and sedimentary denitrification in the Santa Barbara Basin using the stable isotopes of nitrate, *Geochemistry, Geophysics, Geosystems*, 4, <https://doi.org/10.1029/2002GC000384>, 2003.
- Sommer, S., Gier, J., Treude, T., Lomnitz, U., Dengler, M., Cardich, J., and Dale, A. W.: Depletion of oxygen, nitrate and nitrite in the Peruvian oxygen minimum zone cause an imbalance of benthic nitrogen fluxes, *Deep Sea Research Part I: Oceanographic Research Papers*, 112, 113–122, <https://doi.org/10.1016/j.dsr.2016.03.001>, 2016.
- 620 Stevens, E. D.: Use of plastic materials in oxygen-measuring systems, *Journal of Applied Physiology*, 72, 801–804, <https://doi.org/10.1152/jappl.1992.72.2.801>, 1992.
- Stramma, L., Johnson, G. C., Sprintall, J., and Mohrholz, V.: Expanding Oxygen-Minimum Zones in the Tropical Oceans, *Science*, 320, 655–658, <https://doi.org/10.1126/science.1153847>, 2008.
- 625 Strohm, T. O., Griffin, B., Zumft, W. G., and Schink, B.: Growth Yields in Bacterial Denitrification and Nitrate Ammonification, *Applied and Environmental Microbiology*, 73, 1420–1424, <https://doi.org/10.1128/AEM.02508-06>, 2007.
- Thamdrup, B. and Dalsgaard, T.: Production of N<sub>2</sub> through Anaerobic Ammonium Oxidation Coupled to Nitrate Reduction in Marine Sediments, *Appl. Environ. Microbiol.*, 68, 1312–1318, <https://doi.org/10.1128/AEM.68.3.1312-1318.2002>, 2002.
- Thunell, R. C.: Particle fluxes in a coastal upwelling zone: sediment trap results from Santa Barbara Basin, California, *Deep Sea Research Part II: Topical Studies in Oceanography*, 45, 1863–1884, [https://doi.org/10.1016/S0967-0645\(98\)80020-9](https://doi.org/10.1016/S0967-0645(98)80020-9), 1998.
- 630 Tiedje, J. M., Sexstone, A. J., Myrold, D. D., and Robinson, J. A.: Denitrification: ecological niches, competition and survival, *Antonie van Leeuwenhoek*, 48, 569–583, <https://doi.org/10.1007/BF00399542>, 1983.
- Townsend-Small, A., Prokopenko, M. G., and Berelson, W. M.: Nitrous oxide cycling in the water column and sediments of the oxygen minimum zone, eastern subtropical North Pacific, Southern California, and Northern Mexico (23°N–34°N), *Journal of Geophysical Research: Oceans*, 119, 3158–3170, <https://doi.org/10.1002/2013JC009580>, 2014.
- 635 Valentine, D. L., Fisher, G. B., Pizarro, O., Kaiser, C. L., Yoerger, D., Breier, J. A., and Tarn, J.: Autonomous Marine Robotic Technology Reveals an Expansive Benthic Bacterial Community Relevant to Regional Nitrogen Biogeochemistry, *Environ. Sci. Technol.*, 50, 11057–11065, <https://doi.org/10.1021/acs.est.6b03584>, 2016.
- 640 Vonnahme, T. R., Molari, M., Janssen, F., Wenzhöfer, F., Haeckel, M., Titschack, J., and Boetius, A.: Effects of a deep-sea mining experiment on seafloor microbial communities and functions after 26 years, *Science Advances*, 6, eaaz5922, <https://doi.org/10.1126/sciadv.aaz5922>, 2020.
- Yousavich, D. J., Robinson, D., Peng, X., Krause, S. J. E., Wenzhöfer, F., Janssen, F., Liu, N., Tarn, J., Kinnaman, F., Valentine, D. L., and Treude, T.: Marine anoxia initiates giant sulfur-oxidizing bacterial mat proliferation and associated

645 changes in benthic nitrogen, sulfur, and iron cycling in the Santa Barbara Basin, California Borderland, *Biogeosciences*, 21, 789–809, <https://doi.org/10.5194/bg-21-789-2024>, 2024.

Zehr, J. P.: New twist on nitrogen cycling in oceanic oxygen minimum zones, *Proceedings of the National Academy of Sciences*, 106, 4575–4576, <https://doi.org/10.1073/pnas.0901266106>, 2009.

650 Zhang, L., Altabet, M. A., Wu, T., and Hadas, O.: Sensitive Measurement of  $\text{NH}_4^+$   $^{15}\text{N}/^{14}\text{N}$  ( $\delta^{15}\text{NH}_4^+$ ) at Natural Abundance Levels in Fresh and Saltwaters, *Anal. Chem.*, 79, 5297–5303, <https://doi.org/10.1021/ac070106d>, 2007.

Zopfi, J., Kjær, T., Nielsen, L. P., and Jørgensen, B. B.: Ecology of *Thioploca* spp.: Nitrate and Sulfur Storage in Relation to Chemical Microgradients and Influence of *Thioploca* spp. on the Sedimentary Nitrogen Cycle, *Applied and Environmental Microbiology*, 67, 5530–5537, <https://doi.org/10.1128/AEM.67.12.5530-5537.2001>, 2001.

Zumft, W. G.: Cell biology and molecular basis of denitrification., *Microbiol. Mol. Biol. Rev.*, 61, 533–616, 1997.

655